Available online at www.sciencedirect.com

ScienceDirect

Procedia Chemistry 1 (2009) 891–894

Procedia Chemistry

www.elsevier.com/locate/procedia

Proceedings of the Eurosensors XXIII conference

Dipole source localisation using bio-mimetic flow-sensor arrays

A.M.K. Dagamseh*, T.S.J. Lammerink, C.M. Bruinink, R.J. Wiegerink and G.J.M. Krijnen

MESA+ & Impact Research Institutes, University of Twente, Enschede, The Netherlands

Abstract

Flow sensor arrays can be used to extract spatio-temporal flow signatures rather than average or local flow quantities. We look at the equivalent of a fish lateral-line sensor array in air and assess the ability of our artificial hairs flow-sensor arrays to detect flow velocity distributions generated by a vibrating sphere. The measured flow patterns along a virtual lateral-line, carried out over a bandwidth of 0.3 Hz, are found to be in excellent agreement with theory and are used successfully to demonstrate source-distance determination.

Keywords: Hair flow-sensors; Artificial lateral-line; Source localization.

1. Introduction

In nature flow sensor arrays, consisting of a few or larger numbers of sensors distributed in specific geometries, enable the ability to determine object properties by reconstruction from the flow fields generated by mutual velocity. There are various examples of highly-sensitive hairs, arranged in array structures assisting animals to survive and form specific defence mechanism. Crickets [1], spiders [2], scorpions [3] and fish [4] all have flow-sensors in the form of hairs or (in cupula embedded) cillia that detect tiny fluid movements assisting them in locating preys and avoiding predators even in noisy environments. Specifically, the lateral-line in fish has received great attention in the literature to understand the source localization process in fish [5].

Many efforts have been made to understand the localization and tracking of moving objects by detection and reconstruction of flow patterns as performed by lateral-line systems [6]. Theoretical models were made to investigate and describe the stimulus localization mechanisms [7]. These models are based on describing the interactions between the lateral-line organs and the fluid surrounding by applying and solving the Navier-Stokes equation [8]. Since the characteristics of dipole sources are well-known from literature [9], a vibrating sphere generating a dipole velocity field can be conveniently used to analyse object – sensor-array interactions. Once the

* Corresponding author. Tel.: +31-53- 489-2811; fax: +31-53- 489-3343.
E-mail address: a.m.k.dagamseh@ewi.utwente.nl.

1876-6196/09/$– See front matter
doi:10.1016/j.proche.2009.07.222

dipole field-characteristics are determined, information about the source can be retrieved. In an ideal fluid, a sphere vibrating parallel (//) and perpendicular (⊥) to a linear array line, chosen to be parallel to the *x*-axis, generates a flow velocity in the direction of the *x*-axis with amplitudes [9]:

$$V_{x,//}(x) = s\,\omega a^3 \frac{\left(2x^2 - D^2\right)}{\left(x^2 + D^2\right)^{5/2}} \qquad \text{and} \qquad V_{x,\perp}(x) = s\,\omega a^3 \frac{D\,x}{\left(x^2 + D^2\right)^{5/2}} \qquad (1)$$

where ω: angular vibration frequency, a: sphere diameter, s: sphere displacement amplitude and D: distance between the centre of the sphere and sensor reference line (*x*-axis). Fig. 1 shows the velocity profile of a vibrating sphere and fig. 2 shows the parallel and the perpendicular velocity components, at the position of the lateral-line as a typical receptive field plots.

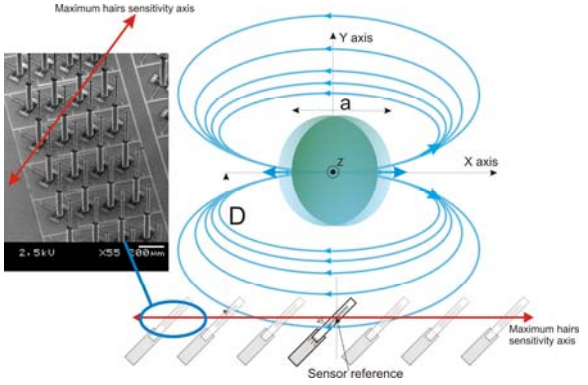

Fig. 1: Sketch for the dipole velocity field and measurements setup. The maximum sensitivity axis of the hair sensor is aligned to be parallel with the x-axis.

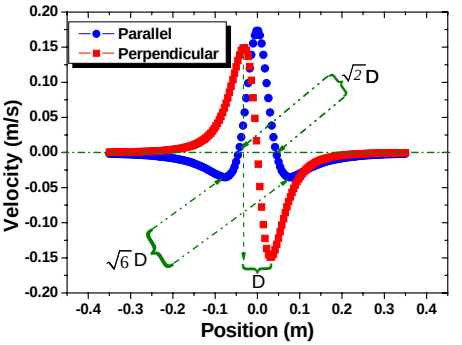

Fig.2: Simulated velocity amplitude V_x as function of sensor position along the x-axis (the parallel and perpendicular components).

The velocity profile is characterised by three peaks separated by two 180° phase shifts for the parallel component plot while the perpendicular component plot has two sequential peaks separated by a 180° phase shift. The velocity components uniquely encode the distance to the source irrespective of the fluid properties, vibration frequency, amplitude, direction and dimensions of the moving object [7][10]. Inspection of equation (1) shows that:

- the two *x* values for which $V_{x,//}(x) = 0$ equal $\pm D/\sqrt{2}$;
- the $V_{x,//}(x)$ has three extrema: one maximum at x = 0 and two minima at $\pm D/\sqrt{2/3}$;
- the $V_{x,\perp}(x)$ has two extrema, a maximum and a mimimum at $\pm D/2$.

Hence the distance D can be determined in various ways: for $V_{x,//}$ the distance between the two zeros equals $\sqrt{2}D$ and the distance between the two minima is $\sqrt{6}D$ while for the $V_{x,\perp}$ the distance between the maxima and minima equals D. Depending on signal to noise ratio and orientation of the sensors the most suitable method can be chosen.

Recently engineering took inspiration from biology to fabricate sensitive micro-mechanical sensing systems surpassing performance of traditionally-engineered sensor system [11]. Fabricating such hairs flow-sensors facilitate both the study of real biological systems and possible applications in engineering contexts. The motivation in this work is to develop an artificial lateral-line mimicing the source localisation function of superficial neuromast of fish. The ability of our hair flow-sensor in determining the flow field is examined by the accurate localization of a vibrating dipole source.

2. Hair-sensor design

In this study, we used an artificial hair flow-sensor inspired by biology [11]. Our sensor was fabricated using sacrificial poly-silicon surface micro-machining technology to form a suspended silicon nitride membrane with ≈ 1

mm long SU-8 hair on top. The hairs maximum sensitivity axis is aligned with a 45^o tilting angle from the *x*-axis. Aluminium electrodes were integrated to form the sensor capacitors. Due to the viscous drag torque acting on the hairs, the membrane tilts and in consequence to that the capacitors, on both halves of the sensor, change equally but oppositely. These capacitive changes are measured differentially to provide measurements for air flows surrounding the hair. A picture for the artificial hair sensor as inspired by crickets is shown in fig. 1.

3. Experimental setup and results

The velocity field generated by a dipole source is detected by a virtual linear array of hair flow sensors. Using one sensor, its position shifted along the *x*-axis with about 3 mm steps, an array with controlled distance *D* from the sphere is constructed. The experimental setup, the definition of distance *D* and the reference coordinate points at the sensor and sphere positions are shown in fig 1.

We investigated the effect of different source parameters to determine the field characteristics needed for the source distance estimation. The model predictions were confirmed by the experimental data. The results for each distance (*D*) in the *y*-direction were plotted as function of position in the *x*-direction along the virtual lateral-line to re-produce the velocity field at each position. The asymmetry in the parallel component plots can be due to the non-zero angle between the vibration axis of the sphere and the sensitivity axis of the hair sensor. We plotted D_{est} as function of *D* to compare the effect of different source parameters on the source localisation. The whole procedure done on the parallel component is applicable for the perpendicular component with D_{est} the distance between the peaks of the plot. A typical dipole velocity-fields (the parallel and perpendicular components) at a distance of *D*=0.056 m (theoritical and measurements) are shown in fig. 3. We investigated the effect of varying the distance (*D*) on the characteristic points of the velocity profiles. Fig. 4 shows the parallel velocity field component while varying *D* and maintaining fixed source vibration conditions. The peak velocity in the *x*-direction has a maximum at the closest position to the sphere and decreases while increasing *D*. The effect of the source vibration frequency and sphere diameter on the detected parallel components at same *D* was investigated and the results are shown in fig. 5. The velocity amplitude has also a maximum at the closest position to the source and gradually decreases while decreasing both the vibration frequency and the sphere diameter and incraesing the distance from the vibrating sphere. A linear relationship (shown in fig. 6) is obtained between *D* and D_{est} for different vibration conditions.

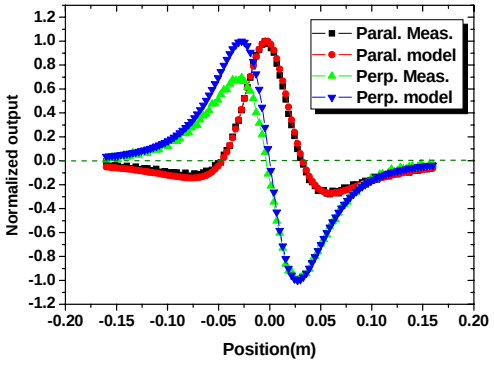

Fig. 3: A typical (measured and simulated) dipole velocity-field (the parallel and perpendicular components) at a distance of D=0.056 m with the same vibration conditions.

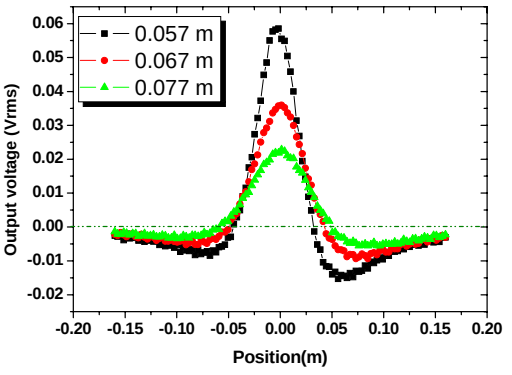

Fig. 4: The parallel velocity field component while varying D and maintaining fixed source vibration conditions.

4. Discussions and conclusions

Inspired by biology we have shown the ability of our hair flow-sensor to reconstruct the velocity field generated by a dipole source. The results show that the dipole source position is encoded in the velocity field along the (virtual) lateral-line system. The sphere diameter, vibrating amplitude and frequency have no influence on the

characteristic points of the velocity field and hence the source localisation procedure is relatively robust. The distance from the source is the only parameter determining the characteristic points of the velocity field. The precision of the source localization is dependent on the determination of the characteristic points (i.e. peak magnitudes and zero crossings) and whether we have a sufficient signal to noise ratio to allow reliable measurements. With the capability of the hair flow-sensor to re-construct the dipole field, we are convinced that our sensors, used in linear array structures, will be able to detect the fields generated by various sources and hence to be used in flow pattern recognition.

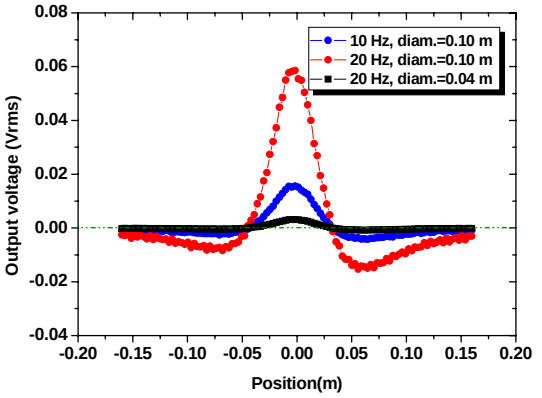

Fig. 5. Effect of the source vibration frequency and sphere diameter on the detected parallel components.

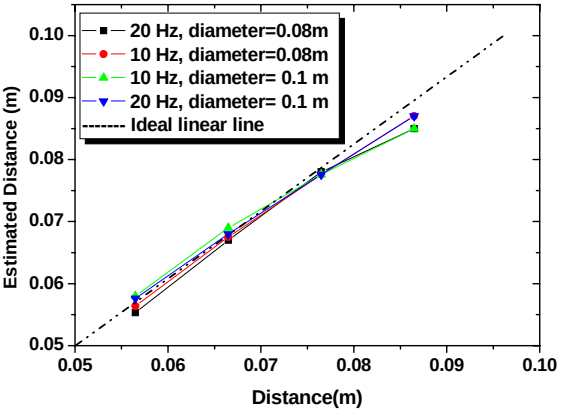

Fig.6: Linear relation between D and D_{est} for different vibration conditions.

Acknowledgments

This research was made possible by grants from the Customized Intelligent Life-Inspired Arrays project funded by the Future and Emergent Technologies arm of IST Programme of the EU and the Bio-Ears Vici grant of the Dutch Technology Foundation (STW/NWO).

References

[1] T. Shimozawa J. Murakami and T. Kumagai, *Cricket wind receptors: thermal noise for the highest sensitivity known*, Chapter 10 in *Sensors and sensing in biology and engineering*, ed. (Barth, Hamphry and Coombs) Springer, Vienna, ISBN 3-211-83771-X (2003).

[2] J.T. Albert, O.C. Friedrich, H.E. Denchant and F.G. Barth, *Journal of Comparative Physiology*; **A187** (2001) pp. 303-12.

[3] W. Sturzl R. Kempter and J.L. van Hemmen, *Physical review letters*; **84** (2000) pp. 5668-71.

[4] S. Coombs, *Autonomous Robots;* **11** (2001) pp. 255-61.

[5] B.C. Blake and S.M. van Netten, *Journal of Experimental Biology.* **209** (2006) pp. 1548–59.

[6] S. Dijkgraaf, *Biological Reviews;* **38** (1963) pp. 51-105.

[7] J-MP Franosch, A.B. Sichert, M.D. Suttner and J.L. Van Hemmen, *Biological Cybernetics*; **93** (2005) pp. 231-8.

[8] D. Acheson, *Elementary fluid dynamics*, Oxford university press, Oxford (1990).

[9] H. Lamb, *Hydrodynamics*, 6th edn. Cambridge University Press, Cambridge, (1932).

[10] J.L. Van Hemmen, private communications, May 2009.

[11] M. Dijkstra, JJ. Van Baar, R.J. Wiegerink, T.S.J. Lammerink, J.H. De Boer and G.J.M. Krijnen, *J. Microelectronics and Microengineering*; **15** (2005) pp. S132-8.